Optical Materials 64 (2017) 126–130

Contents lists available at ScienceDirect

Optical Materials

journal homepage: www.elsevier.com/locate/optmat

Photonic band gap spectra in Octonacci metamaterial quasicrystals

E.R. Brandão [a], M.S. Vasconcelos [b, *], E.L. Albuquerque [c], U.L. Fulco [c]

[a] Departamento de Física Terica e Experimental, Universidade Federal do Rio Grande do Norte, 59072-970, Natal, RN, Brazil
[b] Escola de Ciências e Tecnologia, Universidade Federal do Rio Grande do Norte, 59072-970, Natal, RN, Brazil
[c] Departamento de Biofísica, Universidade Federal do Rio Grande do Norte, 59072-970, Natal, RN, Brazil

ARTICLE INFO

Article history:
Received 8 November 2016
Received in revised form
29 November 2016
Accepted 29 November 2016
Available online 7 December 2016

Keywords:
Plasmon-polaritons
Metamaterials
Photonic crystals
Quasicrystals
Optical band gaps

ABSTRACT

In this work we study theoretically the photonic band gap spectra for a one-dimensional quasicrystal made up of SiO_2 (layer A) and a metamaterial (layer B) organized following the Octonacci sequence, where its nth-stage S_n is given by the inflation rule $S_n = S_{n-1}S_{n-2}S_{n-1}$ for $n \geq 3$, with initial conditions $S_1 = A$ and $S_2 = B$. The metamaterial is characterized by a frequency dependent electric permittivity $\varepsilon(\omega)$ and magnetic permeability $\mu(\omega)$. The polariton dispersion relation is obtained analytically by employing a theoretical calculation based on a transfer-matrix approach. A quantitative analysis of the spectra is then discussed, stressing the distribution of the allowed photonic band widths for high generations of the Octonacci structure, which depict a self-similar scaling property behavior, with a power law depending on the common in-plane wavevector k_x.

1. Introduction

The discovery of quasicrystals in 1982 by Shechtman et al. [1] has started a new field in condensed matter physics. They define a new class of neither amorphous nor crystalline structure exhibiting non translational symmetry. Besides, they can be generated by a substitution rule based on two or more building blocks with long-range order [2–4], exhibiting properties of self-similarity in their spectra with an undoubtedly fractal behavior, with a distinct appearance for each chain [5], even for different excitations [6–8]. As a consequence, many theoretical and experimental works have been reported on this subject (for reviews see Refs. [9–11]).

Quasicrystals are a special class of deterministic aperiodic structures [12]. A recent precise definition of quasicrystals with dimensionality d (d = 1, 2 or 3), is that in addition to their possible generation by a substitution process, they can also be formed from a projection of an appropriate periodic structure in a higher dimensional space mD, where $m > d$ [13]. In contrast, structures that are part of other deterministic structures cannot be built in such way, as by instance quasicrystalline structures of Fibonacci type and their generalizations [14–16], as well as systems that obey the Thue-Morse, double-period and Rudin-Shapiro sequences [17,18]. In this context, the one-dimensional Octonacci structure can be considered as a quasicrystal because it can be formed from a projection of a 2D periodic lattice in a straight line with an irrational slope $\sigma = 1 + \sqrt{2}$ [19].

On the other hand, the idea of complex materials in which both the electrical permittivity and the magnetic permeability possess negative real values at certain frequencies has received considerable attention nowadays due to their potential technological application. This idea was born in 1967 when Veselago theoretically investigated the electromagnetic plane-wave propagation in a material whose permittivity and permeability were assumed to be simultaneous negative [20]. In his theoretical study, Velesago showed that for a monochromatic electromagnetic uniform plane wave in such a medium, the direction of the Poynting vector is antiparallel to the direction of the phase velocity, contrary to the electromagnetic plane-wave propagation in conventional simple media. This theoretical complex medium was setting up by Smith, Pendry, and collaborators [21–24]. They have constructed a composite medium that exhibit the anomalous refraction in microwave regime, demonstrating experimentally the negative refraction studied by Veselago. Many research groups all over the world are now studying their various aspects looking for technological applications [25].

Bulk and surface plasmon-polariton have been

* Corresponding author.
E-mail address: mvasconcelos@ect.ufrn.br (M.S. Vasconcelos).

http://dx.doi.org/10.1016/j.optmat.2016.11.051
0925-3467/

experimentally and theoretically studied for many years due to their possible use in novel photonic and sensing applications (for a review see Ref. [26]). In quasiperiodic structures they exhibit collective properties due to the appearance of long range correlations, which are reflected in their fractal spectra, defining a novel description of disorder [27]. The study of the fractal spectra generated by these quasiperiodic structure can help us to understand the global order and the rules that these systems obey at high generation order. By instance, their spectra in Fibonacci quasiperiodic photonic crystal composed by metamaterials, were already the subject of intense research works [28–30].

The aim of this work is twofold: first, we want to extend our previous work on the transmission spectra in Octonacci photonic quasicrystals [31] by considering the photonic band gap spectra arising from the propagation of a plasmon-polariton excitation in these quasiperiodic multilayer structure. Second, we intend to present a quantitative analysis of the results, mainly those related to the allowed photonic band widths, looking for information about their localization and power laws.

This paper is organized as follows: in Section 2, we present the theoretical model based on the transfer matrix approach to set up analitically the plasmon-polariton dispersion relation (bulk and surface modes). The discussion of this dispersion relation for the Octonacci quasiperiodic structure is then depicted in Section 3, together with their localization profiles through the scaling law of their photonic bandwidth spectra. The conclusions of this work are presented in Section 4.

2. Theoretical model

The Octonacci sequence, also known as Pell sequence, can be built from the Ammann-Beenker tiling, which is an octagonal tiling obtained by using a strip projection method (see Fig. 1.18 in Ref. [32]). The name Octonacci comes from *Octo* for orthogonal and *nacci* from the Fibonacci sequence, the oldest example of a quasiperiodic chain. Its quasi-periodicity can be of the type so-called substitutional sequences, and is characterized by the dense pure point nature of its Fourier spectrum, being described in terms of a series of generations that obey peculiar recursion relations. It can also be defined by the growth, by juxtaposition, of two building blocks A (here considered to be SiO_2) and B (a metamaterial), where the nth-stage of the multilayer S_n is given iteratively by the rule [33]:

$$S_n = S_{n-1}S_{n-2}S_{n-1}, \tag{1}$$

for $n \geq 3$, with $S_1 = A$ and $S_2 = B$. The number of the building blocks increases according to the Pell number $P_n = 2P_{n-1} + P_{n-2}$, for $n \geq 3$, with $P_1 = P_2 = 1$. The number of building blocks B divided by the number of building blocks A, in the limit $n \to \infty$, is $\sigma = 1 + \sqrt{2}$. Another way to obtain this sequence is by using the following inflation rule: $A \to B$, $B \to BAB$. Note that this sequence is classified as Pisot-Vijayaraghavan (PV), when we take the negative eigenvalue of the substitution matrix, i e., $\sigma^- = 1 - \sqrt{2}$ [34,35].

Let us consider first the periodic photonic crystal case. The bulk plasmon-polariton dispersion relation is obtained by solving the electromagnetic wave equation for a p-polarized electromagnetic mode, within the layers A and B of the nth unit cell of the layered photonic crystal (see Fig. 1), yielding:

$$\cos(QL) = (1/2)\mathrm{Tr}(T), \tag{2}$$

where $\mathrm{Tr}(T)$ means the trace of a transfer matrix T. The details of this calculation can be found elsewhere [27]. Using these equations, we can show that for the periodic case this dispersion relation is a function of sines and cosines of the wavevectors k_{zA}, k_{zB} and Q, the Bloch wavevector, and the size $L = a + b$ of the unit cell.

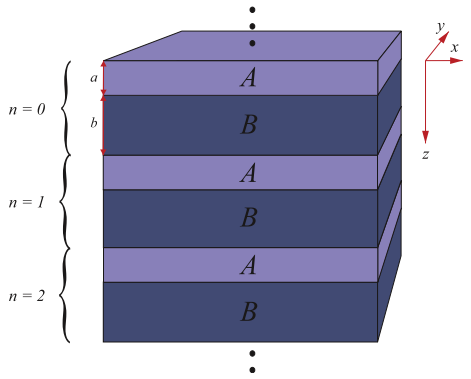

Fig. 1. Schematic representation of a periodic photonic structure $ABAB\cdots$. Here a and b are the thicknesses of the layers A and B, respectively.

To set up the dispersion relation for the surface plasmon-polariton modes, we consider the multilayers structure truncated at $z = 0$, with the region $z < 0$ filled by a transparent medium C, whose dielectric constant is denoted by ε_C. This semi-infinite structure does not present translational symmetry in the z-direction and therefore the Bloch theorem is not valid in this case. Its implicit dispersion relation is [27].

$$T_{11} + T_{12}\lambda = T_{22} + T_{21}\lambda^{-1}, \tag{3}$$

were $T_{ij}\,(i,j = 1,2)$ are the elements of the transfer matrix T, and λ is a surface dependent parameter given by

$$\lambda = (\xi_A + \xi_C)/(\xi_A - \xi_C), \tag{4}$$

$$\xi_j = \varepsilon_j/k_{zj}\,, \tag{5}$$

with $j = C$ or A. Now we extend this method to obtain the plasmon polariton dispersion relation for the Octonacci photonic structure by determining the appropriated transfer matrices. It is easy to prove, by induction method, that the transfer matrices for any Octonacci n-generation (with $n \geq 3$) is given by

$$T_{S_n} = T_{S_{n-1}}T_{S_{n-2}}T_{S_{n-1}}, \tag{6}$$

with the initial conditions

$$T_{S_1} = N_A^{-1}M_A; \quad T_{S_2} = N_B^{-1}M_B. \tag{7}$$

The matrices M_J and N_J ($J = A$ or B) are defined elsewhere [27]. Therefore, from the knowledge of the transfer matrices T_{S_1} and T_{S_2}, we can determine the transfer matrix of any other Octonacci generation.

3. Numerical results

Now we present some numerical results related to the photonic band gap spectra due to the plasmon-polariton excitation (bulk and surface modes) that can propagate in the Octonacci structure considered here. Medium B (A) is a metamaterial (SiO_2) with a frequency dependent (constant) electric permittivity $\varepsilon_B(\omega)$ ($\varepsilon_A = 12.3$) and magnetic permeability $\mu_B(\omega)$ ($\mu_A = 1$) in the

microwave region, defined by Ref. [36]:

$$\varepsilon_B(\omega) = 1 - \omega_p^2 \Big/ \omega^2, \tag{8}$$

$$\mu_B(\omega) = 1 - F\omega^2 \Big/ \left(\omega^2 - \omega_0^2\right), \tag{9}$$

where any damping term, which can be defined as a fraction of the plasma frequency, is neglected. Here the plasma frequency ω_p, the resonance frequency ω_0 and the fraction F are determined only by the geometry of the multilayer system rather than by any other physical parameter like the charge, effective mass and density of electrons. The physical parameters used are $\omega_0/2\pi = 4$ GHz, $\omega_p/2\pi = 10$ GHz and $F = 0.56$, motivated by the experimental work of Smith and collaborators [21]. It is easy to see that for $\omega_0 < \omega < 0.6\,\omega_p$, both the electric permittivity $\varepsilon_B(\omega)$ and magnetic permeability $\mu_B(\omega)$ are negative. Fig. 2 shows the plot of the electric permittivity $\varepsilon(\Omega)$, the magnetic permeability $\mu(\Omega)$, as well as the real and the imaginary part of the refractive index $\eta(\Omega)$ of the metamaterial (medium B), versus the reduced frequency $\Omega = \omega/\omega_p$. As the frequency increases, three important regions have been observed, namely: the white region, in which $\varepsilon_B(\Omega) < 0$ and $\mu_B(\Omega) > 0$, and the yellow (green) region, where $\varepsilon_B(\Omega)$, $\mu_B(\Omega)$ and the refractive index $\eta_B(\Omega)$ are negative (positive).

Fig. 3 depicts the polariton spectrum for a fourth generation quasi-periodic Octonacci structure. The surface modes are represented by full lines, while the bulk modes are characterized by shadow areas. These areas are limited by the constraints $QL = 0$ and $QL = \pi$ in eq. (2). The dashed line represent the vacuum's light line $\omega = ck_x$, while the dot-dashed line is the light line in material A (SiO_2), given by $\omega = ck_x/\varepsilon_A^{1/2}$. The polariton spectrum has well-defined bulk frequency branches, a higher one for $\omega/\omega_p > 1$ and a lower one for $\omega/\omega_p < 1$. They are separated by forbidden frequency gaps, where the surface modes can propagate. For low-frequencies, the bulk branches become narrower when the common dimensionless wavevector $k_x a$ increases, tending asymptotically to the limit value $\omega/\omega_p = 0.3$, here represented by an horizontal dashed line. The high-frequency branch has a parabolic-like form as found

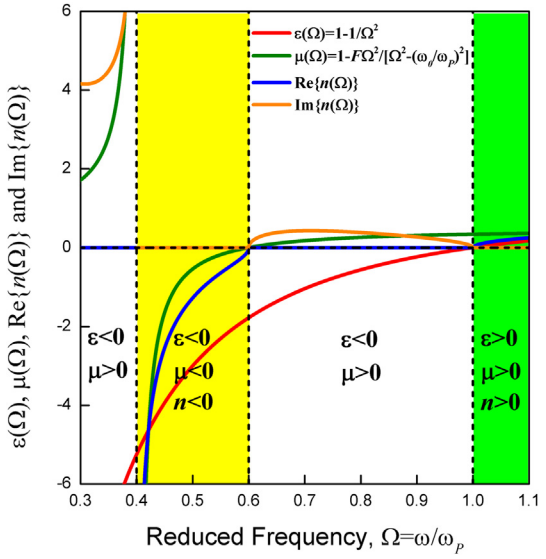

Fig. 2. The electric permittivity $\varepsilon(\Omega)$ (red line), the magnetic permeability $\mu(\Omega)$ (green line), as well as the real (blue line) and the imaginary (orange line) part of the refractive index $\eta(\Omega)$ of the metamaterial (medium B), versus the reduced frequency $\Omega = \omega/\omega_p$. (For interpretation of the references to colour in this figure legend, the reader is referred to the web version of this article.)

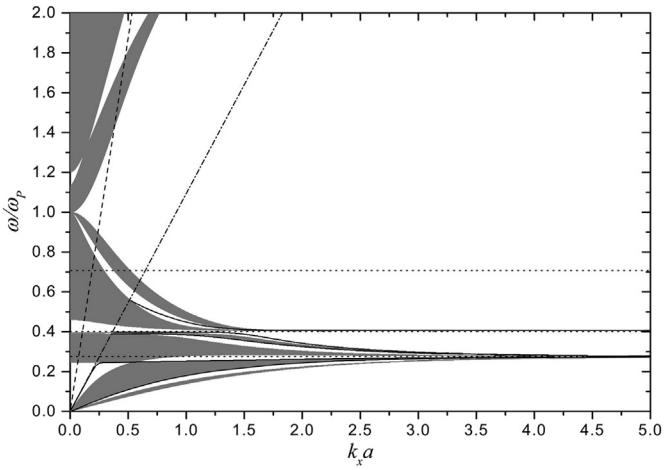

Fig. 3. Polariton spectrum in the fourth Octonacci quasi-periodic sequence. We plot the frequency ω/ω_p as a function of the reduced dimensionless common wavevector $k_x a$. The bulk modes are represented by shaded areas, while the surface modes are represented by straight lines. The dashed line represent the light line in vacuum, while the dot-dashed line is the light line in the layer A (SiO_2). The horizontal dotted lines characterizes frequencies where the polariton modes have asymptotic behavior, namely $\omega/\omega_p = 0.3$ and 0.4.

in positive refractive index materials. The bulk modes localized in the frequency range $0.3 \leq \omega/\omega_p \leq 1.0$, have a negative slope, an interesting negative group velocity characteristic already found previously [28]. Besides, there are three surface modes with negative slope, the so-called backward mode, starting at the light line in layer A. One of them, the more energetically one, tends to $\omega/\omega_p = 0.4$ for high-values of $k_x a$, while the other two tends asymptotically to the limit value $\omega/\omega_p = 0.3$. The other low-frequencies surface modes have positive slope (forward mode), starting on $\omega/\omega_p = k_x a = 0$, and tending to $\omega/\omega_p = 0.3$. Going further, the polariton spectra in a higher generation of the Octonacci quasiperiodic depict, qualitatively speaking, a similar photonic band gap spectra, with the bulk bands now much more fragmented, with a consequent increase of the surface modes, as expected.

Let us now examine the polariton confinement effects due to competition between the long-range aperiodic order, induced by the Octonacci quasiperiodic structure, and the short-range disorder. To do that we employ a quantitative analysis of the localization and magnitude of the allowed frequencies (pass bands) width in the photonic band gap spectra, setting up the regions for allowed frequencies where $|(1/2)\mathrm{Tr}(T)| \leq 1$, as a function of the generation number n of the quasiperiodic structure for fixed values of the common dimensionless wavevector $k_x a$, namely $k_x a = 0.25$ (Fig. 4a), $k_x a = 0.35$ (Fig. 4b) and $k_x a = 0.50$ (Fig. 4c), respectively. We have considered the Octonacci generation number n up to 12, which means a unit cell with 8119 building blocks, being 2378 of SiO_2 (material A) and 5741 of the metamaterial (B blocks). As one can see, the number of pass bands are related to the number of building blocks. Furthermore, when we increase the generation number of the Octonacci structure (higher values of n) the pass bands regions turn more narrowed, leading the bulk bands to become a set of straight modes, such as what occurs in the Cantor fractals.

In order to characterize this fragmentation process, we calculate the total bandwidth Δ, the Lebesgue measure of the energy spectrum, of the allowed frequencies as a function of the generation number n, plotted on a log-log graph in Fig. 5. From there one can see that the pass bands regions decreases as a function of the

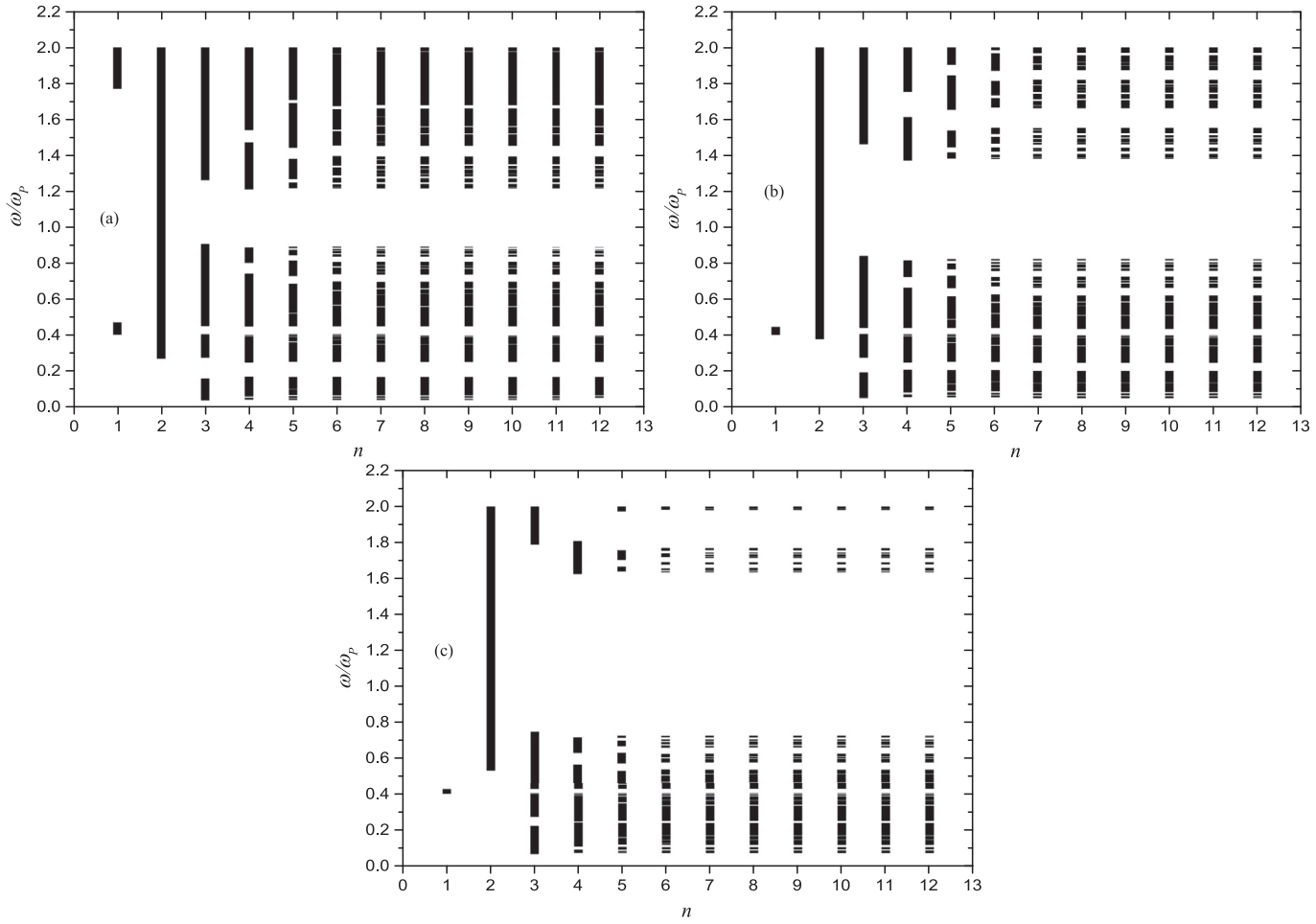

Fig. 4. Localization and scaling properties of the allowed frequencies (pass bands) width in the Octonacci photonic band gap spectrum as a function of the generation number n considering the following values of the common dimensionless wavevector $k_x a$: a) 0.25, b) 0.35, c) 0.50.

number of generation n by a power law $\Delta \sim P_n^{-\delta}$, P_n being the Pell's numbers and the exponent δ, the diffusion constant of the spectra, being a function of the common in-plane wavevector $k_x a$. This exponent can indicate the degree of localization of the excitation [37,38].

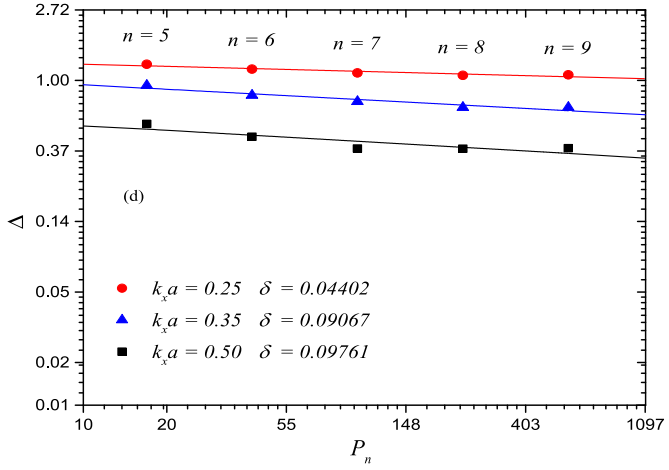

Fig. 5. Log-log plot of the total bandwidth Δ as a function of the Pell's number P_n, considering the common dimensionless wavevector $k_x a$ equal to 0.25 (red dots), 0.35 (blue triangles) and 0.5 (black squares) respectively. (For interpretation of the references to colour in this figure legend, the reader is referred to the web version of this article.)

4. Conclusions

In summary, we have presented a general theory for the propagation of plasmon-polaritons in quasi-periodic photonic crystal following an Octonacci sequence, whose building blocks are made of an insulator (metamaterial) with constant (frequency dependent) refractive index in a given frequency region. The spectrum is illustrated in Fig. 3 depicting not only the effects of the introduction of the negative refractive index material, mainly in the region $0.3 \leq \omega/\omega_p \leq 1.0$ where exists many bulk and surfaces modes with backward behavior, but also the fractality aspect due to the quasi-periodicity of the multilayer system. Besides, in the lowest and highest frequency region of the spectrum the plasmon-polaritons branches show only positive slopes with propagation modes of normal (ordinary) properties, which are characteristic of a material with positive refraction index. Regarding experimental techniques to probe these theoretical predictions, the Raman light scattering spectroscopy in a typical shift of the frequency of the scattered light in the range investigated here is probably the most appropriated one [39].

We have also studied physical properties related to their localization, as expressed by the distribution of the pass bands widths shown in Fig. 4a, b and 4c. Their self-similarity behavior, leading to

a fractal profile, is characterized by the power law depicted in Fig. 5 for three different values of the common dimensionless wavevector $k_x a$, namely $k_x a = 0.25$, $k_x a = 0.35$ and $k_x a = 0.50$, with no counterpart for the periodic case.

Acknowledgements

The authors would like to thank CAPES and CNPq (Brazilian Science Funding Agencies) for the financial support.

References

[1] D. Shechtman, I. Blech, D. Gratias, J.W. Cahn, Phys. Rev. Lett. 53 (1984) 1951.
[2] E.M. Barber (Ed.), Aperiodic Structures in Condensed Matter: Fundamentals and Applications, CRC Press, 2008.
[3] L. dal Negro (Ed.), Optics of Aperiodic Structures: Fundamentals and Device Applications, Pan Stanford Publishing, 2013.
[4] E.L. Albuquerque, U.L. Fulco, V.N. Freire, E.W.S. Caetano, M.L. Lyra, F.A.B.F. Moura, Phys. Rep. 535 (2014) 139–209.
[5] P.M.C. de Oliveira, E.L. Albuquerque, A.M. Mariz, Physica A 227 (1996) 206–212.
[6] E.L. Albuquerque, M.G. Cottam, Solid State Commun. 81 (1992) 383–386.
[7] C.G. Bezerra, E.L. Albuquerque, Physica A 255 (1998) 285–292.
[8] D.H.A.L. Anselmo, M.G. Cottam, E.L. Albuquerque, J. Phys. Condens. Matter 12 (2000) 1041–1052.
[9] E.L. Albuquerque, M.G. Cottam, Polaritons in Periodic and Quasiperiodic Structures, Elsevier, Amsterdam, 2004.
[10] E.L. Albuquerque, M.G. Cottam, Phys. Rep. 376 (2003) 225–337.
[11] E. Maciá, Rep. Prog. Phys. 75 (2012) 036502.
[12] C. Janot, Quasicrystals, A Primer, Oxford Univ. Press, Oxford, 1993.
[13] Z.V. Vardeny, A. Nahata, A. Agrawal, Nat. Photonics 7 (2013) 177–187.
[14] G.Y. Oh, C.S. Ryu, M.H. Lee, Phys. Rev. B 47 (1993) 6122.
[15] C.A.A. Araujo, M.S. Vasconcelos, P.W. Mauriz, E.L. Albuquerque, Opt. Mat. 35 (2012) 18–24.
[16] C.H.O. Costa, M.S. Vasconcelos, J. Phys. Condens. Matter 25 (2013) 286002.
[17] M.S. Vasconcelos, E.L. Albuquerque, A.M. Mariz, J. Phys. Condens. Mat. 10 (1998) 5839–5849.
[18] M.S. Vasconcelos, E.L. Albuquerque, Phys. Rev. B 59 (1999) 11128–11131.
[19] S. Hoffmann, H.R. Trebin, Phys. Stat. Sol. (b) 174 (1992) 309–323.
[20] V.G. Veselago, Sov. Phys. Usp. 10 (1968) 509–514.
[21] D.R. Smith, W.J. Padilla, D.C. Vier, S.C. Nemat-Nasser, S. Schultz, Phys. Rev. Lett. 84 (2000) 4184–4187.
[22] R.A. Shelby, D.R. Smith, S. Schultz, Science 292 (2001) 77–79.
[23] J.B. Pendry, Phys. Rev. Lett. 85 (2000) 3966–3969.
[24] J.B. Pendry, Science 306 (2004) 1353.
[25] S. Johnson, J.D. Joannopoulos, Photonic Crystals: The Road from Theory to Practice, Kluwer, Boston, 2002.
[26] E.L. Albuquerque, M.G. Cottam, Phys. Rep. 233 (1993) 67–135.
[27] M.S. Vasconcelos, E.L. Albuquerque, Phys. Rev. B 57 (1998) 2826–2833.
[28] M.S. Vasconcelos, P.W. Mauriz, F.F. de Medeiros, E.L. Albuquerque, Phys. Rev. B 76 (2007) 165117.
[29] F.F. de Medeiros, E.L. Albuquerque, M.S. Vasconcelos, J. Phys. Condens. Matter 18 (2006) 8737–8747.
[30] S.B. Cavalcanti, M. de Dios-Leyva, E. Reyes-Gómez, L.E. Oliveira, Phys. Rev. B 74 (2006) 153102.
[31] E.R. Brandão, C.H. Costa, M.S. Vasconcelos, D.H.A.L. Anselmo, V.D. Mello, Opt. Mat. 46 (2015) 378–383.
[32] W. Steurer, S. Deloudi, Crystallography of Quasi Crystals, Springer Series in Material Science, Springer-Verlag, Heidelberg, 2009.
[33] H.Q. Yuan, U. Grimm, P. Repetowicz, M. Schreiber, Phys. Rev. B 62 (2000) 15569–15578.
[34] J.P. Lu, T. Odagaki, J.L. Birman, Phys. Rev. B 33 (1986) 4809–4817.
[35] A.G. Barriuso, J.J. Munzón, T. Yonte, A. Felipe, L.L. Sánchez-Soto, Opt. Express 21 (2013) 30039.
[36] H.V. Shadrivov, A.A. Sukhorukov, Y.S. Kivshar, Appl. Phys. Lett. 82 (2003) 3820.
[37] E. Maciá, Rep. Prog. Phys. 69 (2006) 397–441.
[38] P. Hawrylak, J.J. Quinn, Phys. Rev. Lett. 57 (1986) 380.
[39] E.L. Albuquerque, J. Phys. C 13 (1980) 2623–2639.